*Abstracts in this section pertain to papers presented as Works-in-Progress at the 32nd Annual Meeting of the SNM, June 2–5, 1985, at the Albert Thomas Convention Center, Houston, Texas. Scientific Program Chairman: Philip O. Alderson, MD*

**The Use of 15-*p*-(I-123)-Iodophenyl-β-Methylpentadecanoic Acid (BMPDA) for Myocardial Scintigraphy in Man.** R. Dudczak, P. Angelberger, R. Schmoliner, and K. Kletter. *1st Medical Clinic, University of Vienna, Austria.*

Recently 15-*p*-(I-123)-iodophenyl-β-methylpentadecanoic acid (BMPDA) was proposed as myocardial imaging agent as a possible probe of metabolic processes other than β-oxidation.

In 19 patients (CAD, n = 15, St.p.MI/7; controls, n = 4) BMPDA was applied for myocardial scintigraphy. All were studied fasted, supine in the LAO (n = 14) or anterior (n = 5) view. After i.v. BMPDA (2–4 mCi) data were collected for 100 min. From heart (H) and liver (L) organ to background (BG) ratios were calculated and BG (V.cava) corrected time-activity curves analyzed. In ten pts. plasma (P) and urine (U) were examined.

After an initial decrease in P activity there was a slight increase. P extraction showed with time an increase in the activity of the aqueous phase. Thin layer chromatographic (TLC) fractionation of the organic phase showed activity peaks comparable to bencoic acid, BMPDA, and triglycerides. In U 4.1 ± 0.9% dose were excreted within 2 hr; by TLC hippuric acid was found.

In 13 diseased regions (MI/7) BMPDA uptake was reduced. The mean maximal BMPDA uptake in the H was at 15 min and in the L at 9 min with H/BG and L/BG ratios of 1.8 and 2.1, respectively. Elimination (E) was slower from the H than from the L ($p < 0.01$). It was biexponential from the L ($\bar{x}$: t/2 I 11.4 min, t/2 II 91.5 min, t/2 I uncorr. 37.5 min). In the H, turnover was biexponential in 11 pts ($\bar{x}$: t/2 I 13.8 min, t/2 II 187 min, t/2 I uncorr. 65 min), but monoexponential in eight (t/2-218 ± 102 min). The size of phase I was smaller than that of phase II ($\bar{x}$: I/II in H 0.34; I/II in L 0.57). The E behavior was mostly abnormal from diseased myocardial regions as compared to the respective normal region.

Our data show that BMPDA may be useful myocardial imaging agent; its longer myocardial retention compared to unbranched radioiodinated fatty acids may facilitate SPECT studies. Yet, possible catabolic breakdown limits curve interpretation.

**Uptake of Myocardial Imaging Agents by Transplanted Human and Rat Hearts.** J. Bergsland, E.A. Carr, Jr., M. Carroll, J.R. Wright, J.M. Gona, J.N. Bhayana, and M. Montes. *Buffalo VA Medical Center, Buffalo, NY.*

Monitoring of transplanted hearts for rejection now requires frequent biopsies. In 1969 we showed in animals and man that myocardial scintigram with cesium-131 ($^{131}$Cs) detected rejection. We have now studied uptake of technetium-99m ($^{99m}$Tc) pyrophosphate, thallium-201 ($^{201}$Tl) and gallium-67 ($^{67}$Ga), given as citrate, by transplanted rat hearts during rejection. Lewis-Brown Norway $F_1$ rats received heterotopic grafts from syngeneic (SYN) or allogeneic (ALLO) rats (ACl strain). We gave $^{99m}$Tc 2 hr before, and $^{201}$Tl 20 min before killing, or $^{67}$Ga 1 day before killing. Results (n = 7–14/group) expressed as uptake ratios, graft/native heart, were: $^{99m}$Tc at 3 d post-op LV (SYN) = 1.34 ± 0.10 (s.e.m.) compared with LV (ALLO) 1.74 ± 0.16 ($p < 0.05$), RV 1.72 ± 0.20 compared with 1.72 ± 0.19. At 5 d LV = 1.51 ± 0.11 compared with 3.27 ± 0.45 ($p < 0.003$), RV 1.31 ± 0.13 compared with 2.08 ± 0.19 ($p < 0.01$). Ga-67 at 3 days LV = 1.72 ± 0.27 compared with 2.29 ± 0.25 (NS) RV, 2.10 ± 0.33 compared with 3.19 ± 0.70 (NS). At 5 days LV = 1.67 ± 0.55 compared with 3.05 ± 0.17 ($p < 0.05$), RV 1.60 ± 0.29 compared with 3.70 ± 0.34 ($p < 0.005$). All $^{201}$Tl differences were NS. Mean rejection grades (scale 0 to 4) in all ALLO combined were 1.9 at 3 d and 2.5 at 5 days. In all technetium-99m combined, correlation (uptake compared with degree of rejection) was stronger in LV (0.52, $p < 0.001$) than RV (0.21, $p = 0.06$) and linearity was better in LV.

Nine serial myocardial scintigrams of each of two nonrejecting human transplants (1–6 wk and 4–40 wk post-op) showed consistently normal thallium-201 and normal (absent) technetium-99m. Thus healthy human transplants have normal baseline uptakes, and rat data suggest technetium-99m and gallium-67 may detect rejection; $^{99m}$Tc appears more sensitive.

**Follow-Up of Acute Myocardial Infarction by Thallium-201 Scores for Extent and Severity.** A. Franke and K. Oeff. *Department of Nuclear Medicine, Klinikum Steglitz, Free University of Berlin, Berlin, F.R.G.*

Profiles of relative distribution of thallium-201 ($^{201}$Tl) in the myocardium were evaluated in 30 patients (21 males, age 41–74 yr, mean 54 yr, and nine females, age 38–72 yr, mean 61 yr) within 6 hr of onset of acute myocardial infarction (AMI). These patients were subjected to a randomized double-blind study of the efficacy of streptokinase (SK) thrombolytic therapy. Thallium-201, 74 MBq, was injected 1.9 ± 1.6 hr after the intravenous injection of SK or placebo. Scintigraphy was performed employing the seven pinhole tomographic reconstruction technique developed by Vogel et al. [*J Nucl Med* 19: 648–654, 1978; *Am J Cardiol* 43: 787–793, 1979; *IEEE Trans Nucl Sci* 27: 412–420, 1980]. Each study was evaluated by quantitative analysis of the circumferential profiles (CPs) of the initial $^{201}$Tl uptake (1.0 ± 0.9 hr after tracer injection) and the 24-hr clearance rates generated by each of six left-ventricular short-axis tomographic sections (distance between planes = 1 cm), two slices each representing the apical, mid-ventricular and basal left-ventricular sections. The CPs were constructed by the computer from the values of 60 radii spaced at 6° intervals plotted anticlockwise. Each CP was normalized to the maximum value found for that profile. Abnormal Tl-201 distribution or washout was identified by comparison of the CP for each patient with the corresponding sex-related limits of normal CPs. Normal CPs

were obtained in 20 patients considered as normals by coronary arteriography, ventriculography and cardiac catheterization under exercise. Thallium-201 scores for quantification of the extent and severity of perfusion defects and washout abnormalities were obtained by calculating the number of abnormal segments (total n = 72) and (2) the sum of % deviation from the normal limits. The follow-up of disease was evaluated by $^{201}$Tl scintigraphy following stress and subsequent washout which was performed 3 wk to 12 mo after AMI.

A significant reduction of the extent and severity as determined by $^{201}$Tl scores was observed between initial and 24-hr delayed images. A similar reduction was also observed in follow-up measurements between initial stress and 3-hr delayed images. The changes in extent and severity for both measurements are indicative of considerable ischemia of the infarcted area. Preliminary evaluation of the effect of SK compared with placebo in 24 patients revealed a slight reduction in the severity of $^{201}$Tl defects and an increase in percent recovery within 24 hr of onset of AMI in the SK group. No significant differences were observed in males and females as well as in anterior and posterior wall involvement.

**Evaluation in Man and Dog of Three New Cationic Technetium-99m Complexes for Myocardial Perfusion Imaging.** P. Gerundini, E. Deutsch, A. Savi, M.C. Gilardi, L. Zecca, W. Hirth, K. Libson, and F. Fazio. *University of Cincinnati, Cincinnati, OH and Instituto San Raffaele, Milano, Italy.*

The cationic technetium-99m complexes $[^{99m}Tc(TMP)_6]^+$, $[^{99m}Tc\text{-}(POM\text{-}POM)_3]^+$ and $[^{99m}Tc(TBIN)_6]^+$, where TMP = trimethylphosphite, POM-POM = 1,2-bis(dimethoxyphosphino)ethane, and TBIN = *tert*-butylisonitrile, have been studied as myocardial perfusion imaging agents in dog and man. Each agent was prepared from "no carrier added" $^{99m}TcO_4^-$ in greater than 93% radiochemical purity and was injected into dogs and at least three human volunteers. Activity was recorded on a computerized gamma camera, and serial blood samples were collected. In dogs, blood clearance is fast for all three complexes ($t_{1/2}$ of first component = 1.5 min for the TMP complex, 1.5 min for the POM-POM complex, and 1.0 min for the TBIN complex) and good quality myocardial images are obtained within 1 hr after injection. In man, blood clearance for the TMP and POM-POM complexes is slow ($t_{1/2}$ = 38 and 33 min, respectively), the resulting low myocardium/blood-pool ratio preventing the acquisition of myocardial images until 4–6 hr after injection. Even at that time, the images are poor and suffer from lung and liver background. The TBIN complex shows a faster blood clearance ($t_{1/2}$ = 1 min) and early concentration of activity in the heart wall, but the initially high lung background allows acceptable heart images to be obtained only 1–3 hr after injection. While the TBIN complex clearly provides the best myocardial images, none of the agents studied appear suitable for routine clinical use. The dog is not an adequate model for evaluation of cationic $^{99m}$Tc complexes designed for myocardial perfusion imaging.

**Evaluation of Developmental Hemodynamics in a Mini Swine Model of Congenital Heart Disease Using Serial Cardiovascular Nuclear Medicine Techniques.** L.A. Latson, R.A. Stratbucker, M.A. Quaife, K.L. Kilzer, R.F. Kelly. *University of Nebraska Medical Center, Omaha, NE.*

Noninvasive nuclear medicine (NM) methods were employed in two groups of young mini swine characterized as (a) shunt surgery controls, and (b) surgically created left to right central shunts (SH). SH were either externally controllable by a pneumatic occluder encircling tubular grafts or fixed direct anastomoses between the aorta and main pulmonary artery. NM studies were performed using technetium-99m-($^{99m}$Tc) labeled autologous red blood cells injected as a tight bolus deriving values for Qp/Qs ratios plus RVEF's & LVEF's from corresponding region of interest (ROI) time-activity curves. Gated equilibrium studies were obtained after a 15-min delay. Both LVEF and RVEF were calculated from smoothed images using semi-automatic edge detection. Unique porcine anatomy dictated left lateral views for optimal pulmonary ROI's and 40° LAO views for optimal ventricular separation. To date 36 studies have been completed in 12 mini swine and grouped as shown below.

| | Age (mo.) | # | SH | RVEF | LVEF | Qp/Qs |
|---|---|---|---|---|---|---|
| Group 1 | 2–4 | 7 | – | 34 ± 4 | 46 ± 7 | 1.05 ± 0.0 |
| Group 2 | 2–4 | 7 | + | 35 ± 6 | *37 ± 9 | *2.56 ± 0.0 |
| Group 3 | 4–10 | 22 | – | 43 ± 7 | *57 ± 13 | *1.1 ± 0.1 |

[mean + 1 s.d.* = Significant difference with $p < 0.05$]

These results suggest that RVEF and LVEF are significantly lower in pigs 2–4-mo-old compared to pigs 4–10-mo-old. LVEF is even lower in young pigs with a patent shunt but not significantly different from control young pigs.

**Improved Detection of Regional Wall Motion Abnormalities by Factor Analysis of Radionuclide Gated Studies.** D.G. Pavel, J. Sychra, K. Zolnierczyk, C. Kahn, S. Virupannavar, E. Olea, and J. Shanes. *University of Illinois, Chicago, IL.*

Factor analysis (FA) was evaluated in comparison with amplitude (A) and phase analysis (PhA) on 13 normals (N1) and 36 patients in which biplane contrast angiography was available. In 16/36 Tl-201, surgery or autopsy were also available. The basic algorithm was similar to recently published method (Cavailloles et al.) but optimized for regional wall motion abnormalities (RWMA) detection. Only ventricular regions of interest independently obtained from optimized LAO views were used as input data. These were processed and submitted to a search for 2 and 3 factors (F). N1: the 2F search showed in all 13 a well-defined ventricular F (VF) image similar to the A image; the second F was of relatively ill-defined nature eliciting LV base and also delineating the pulmonary outflow tract area. The 3F search failed to generate significant information in the third F image. Pts: 13/14 cases with dyskinesia (Dys) had VF image of 2F display different than A. Overall the combined 2F and 3F displays correlated as follows: (a) for number of locations within a ventricle having RWMA, FA was better than phase analysis in 33/36 (93%), (b) for type of maximum abnormal-

ity found in each respective case FA was better in 27/36 (75%). FA was worse in only 1/36. This improvement was particularly striking for septal abnormalities, for small Dys areas, for multiple RWMA and for large areas of hypokinesia. In conclusion by optimizing the technique and applying it to ventricular areas only, FA improves significantly the detection of RWMA, (better than recently described in literature) especially for locations notoriously difficult to evaluate otherwise.

**Early Clinical Experience with the Interpretation of Medical Images by an Artificial Intelligence Expert System.** W. A. Erdman, C. Helm, T.J. Stahl, P. Lewis, J. Gronlund-Jacob, and D. Rao. *UMDNJ-Rutgers Medical School, Middlesex General-University Hospital, New Brunswick, NJ.*

We have been developing a Medical Image Decision Assistance System (MIDAS) which creates an interpretive report and a diagnostic impression using a computerized analysis of features extracted from nuclear medicine images. The current MIDAS programs create reasonable interpretations of the results of gated blood-pool exams using comparisons of features extracted from patient image data with corresponding features from a normal population. There is some evidence that clinically important abnormalities and relations which can be missed during a visual analysis can be picked up by MIDAS. We use an AI EXPERT system (currently running on a DEC-20) for initial design and debugging. The models are then cross-compiled into FORTRAN and loaded in the nuclear medicine Sperry Univac V77-600 computer for execution. We are evaluating cases prospectively and retrospectively using comparisons with independent clinical interpretations and angiographic findings when available. Our impression is that artificial intelligence evaluations of at least some medical images is a practical possibility in current clinical situations.

**Automatic Region-of-Interest Definition for Normal Liver Volume Calculation and Spleen Region Deletion in SPECT.** J.R. Wallace, N.C. Yang, P.K. Leichner, T.L. Frankel, W.G. Hawkins, and D.M. Loudenslager. *The Johns Hopkins Oncology Center, Baltimore, MD.*

Liver volumes were calculated for ten patients with primary hepatic tumors using computerized contouring of the normal liver region in transaxial slices generated by single-photon emission computed tomography (SPECT). The imaging agent used was technetium-99m ($^{99m}$Tc) sulfur colloid.

Prior to volume calculation, the spleen region was automatically identified and deleted in each set of images using thresholding and region growing techniques. Normal liver regions were then obtained by thresholding each image at a percentage of the maximum count in the liver and volumes determined by multiplying region areas by slice thickness and summing over the set of contiguous slices. The resulting volumes were compared with normal liver volumes obtained from computed tomographic (CT) scans. The best threshold overall was determined to be 46%, for which the correlation coefficient was 0.81.

The liver regions derived from SPECT and CT images were then compared in detail using software developed to overlay the two types of images. Based on these comparisons, it is apparent that a single threshold is not appropriate for all patients. Currently, an attempt is being made to incorporate [$^{99m}$Tc] sulfur colloid uptake in the liver into the determination of a unique threshold for each patient.

**Is Sodium Iodide Iodine-123 the Thyroid Imaging Agent of Choice? A Dosimetric Evaluation.** H.A. Ziessman and F.H. Fahey. *Georgetown University Medical Center, Washington, DC.*

The thyroid radiation absorbed dose (RAD) of iodine-123 ($^{123}$I) was determined at various ages using recommended administered activities at the time of delivery (TOD) and at 2 half-lives ($T_{1/2}$). Iodine-123 is considered by many as the radionuclide of choice for thyroid scintigraphy, especially children. The RAD/$\mu$Ci of pure $^{123}$I is considerably lower than $^{131}$I and almost as low as technetium-99m. However, commercially available iodine-123 (p,2n) and more recently (p,5n) have contaminants of iodine-124 and iodine-125, respectively. The availability of only 100 $\mu$Ci capsules makes the administration of recommended activities for children difficult. The capsule must be "decayed down" or a larger than recommended activity administered.

The MIRD formalism was used to estimate the RAD based on recommendations of administered activities at various ages (*J Nucl Med* 19:207, 1978) and assuming radio-contamination levels (at TOD) as specified by the suppliers.

The thyroid RAD per administered activity for $^{123}$I produced through (p,2n) is five times that of pure $^{123}$I with a scan dose ranging from 11 (adult) to 25 (age 1) rad and twice that from (p,5n) production. These (p,2n) RADs are 9–11 times that of a $^{99m}$Tc scan. The RAD from a (p,2n) scan is considerably higher than that for a combined $^{99m}$Tc scan and $^{131}$I uptake (Tc-IU) study, and even (p,5n) only yields a RAD advantage over Tc-IU at age $\leq$1 yr. If the lower pediatric administered activities are achieved by allowing the radionuclide to decay for 2 T½s, then the RAD from a (p,2n) scan is 30–70 rad and (p,5n) is higher for all ages except the newborn, due to the relative increase in the long-lived radiocontaminants. In conclusion there is no dosimetric advantage of commercially available $^{123}$I for thyroid scintigraphy for adults and most children.

**Esophageal Emptying in Esophageal Disorders.** A. Singh, G.J. Wang, R.A. Holmes, J. Butt, and S. Welch. *V. A. H. and University of Missouri, Columbia, MO.*

Radionuclide esophageal emptying studies were performed to assess the severity and frequency of esophageal motor dysfunction (EMD) in 53 patients with proven esophagitis, Barrett's esophagus, hiatal hernia (HH) with or without reflux and achalasia. After an overnight fast the subjects were placed supine beneath the camera and asked to swallow a 15 ml bolus of water containing 1 mCi of technetium-99m sulfur colloid with dry swallows on command every 15 sec for 4 min. Using computer, esophageal emptying (EE) was calculated, EE = [(EMax − Et) ÷ EMax]100; where EMax is peak count rate and Et is count rate at time t. Values <2 s.d. below mean were interpreted as abnormal. Comparisons were made using Mann-Whitney test ($p < 0.05$). The results are given below.

| Condition | No. of sub | Esophageal emptying 15 sec mean | 15 sec s.d. | 60 sec mean | 60 sec s.d. | 120 sec mean | 120 sec s.d. |
|---|---|---|---|---|---|---|---|
| Normal | 7 | 93.8 | 4.5 | 96.6 | 0.5 | 98.1 | 0.7 |
| Esophagitis | 19 | 67.3 | 36.4 | 78.3 | 27.6 | 84.8 | 22.7 |
| Barrett's | 13 | 63.9 | 30.5 | 76.4 | 26.6 | 82.7 | 22.9 |
| HH with reflux | 5 | 67.2 | 34.0 | 72.9 | 37.1 | 80.1 | 29.7 |
| HH w/o reflux | 13 | 63.1 | 32.7 | 70.6 | 27.3 | 82.4 | 23.4 |
| Achalasia | 3 | 44.8 | 26.6 | 53.2 | 34.3 | 58.9 | 40.0 |

In conclusion: 1. Esophagitis, Barrett's esophagus, and hiatal hernia were associated with similar degree of EMD and patterns of emptying were indistinguishable. EMD was most severe in achalasia. 2. Presence or absence of reflux did not correlate with EMD in HH patients. 3. The frequency of EMD was 42% in esophagitis, 62% in Barrett's esophagus, 55% in hiatal hernia and 100% in achalasia.

**Experimental Studies of Platelet Adhesion and Flow Characteristics in Synthetic Grafts Utilizing Scintillation Camera and NMR Techniques.** H. Pärsson, B-A Jönsson, F. Stahlberg, L. Norgren, B. Persson, J. Thörne, and S-E Strand. *Depts. Surgery and Radiation Physics, Lund University, Sweden.*

Factors with influence on graft patency in arterial reconstructive surgery are, among others, thrombogenicity and different flow parameters.

In anesthetized pigs the femoral arteries are dissected bilaterally and grafts of 4 cm length are inserted end to side. The intermediate artery is ligated. Immediately after operation indium-111- ($^{111}$In) labeled autologous platelets are injected, and continuous measurement over the grafts performed for 3 hr show accumulation in the grafts of $^{111}$In platelets.

The mean blood flow rate in the same kind of grafts is then measured in vitro with a 0.25T nuclear magnetic resonance (NMR) analyzer by means of the inflow-outflow method.

The study hitherto shows that the methods utilized give good possibility to investigate different graft characteristics. NMR studies will be completed in vivo in a 0.15T NMR scanner, built at the department, using the same animals as for the platelet studies.

**Formaldehyde Fixed Cells Compared with Live Cells for Antibody Immunoreactivity Assay.** P.L. Beaumier, D.F. Neuzil, H.M. Yang, E.A. Noll, K.A. Krohn, I. Hellstrom, K.E. Hellstrom, and W.B. Nelp. *Oncogen and the University of Washington, Seattle, WA.*

To avoid repeated culturing and harvesting of live cells we developed a convenient and reproducible antibody cell binding assay using fixed cells. The assay is used routinely to test the immunoreactivity of monoclonal antibodies (Mab) and fragments (Fab) after iodination, prior to clinical use. A human melanoma cell line (M2669 CL13) was selected, by immunofluorescence screening, from a panel of cultured cloned lines that expressed high levels of 3 specific melanoma-associated antigens; p97, proteoglycan and GD3 ganglioside. Cultured cells were detached using EDTA and fixed in 3% paraformaldehyde in PBS for 15 min at room temp., then washed and stored at 4°C. Under standard assay conditions, about 1 ng of I-125 labeled Mab or Fab diluted in 100 $\mu$l of fetal calf serum was incubated with $5 \times 10^6$ cells for 30 min at room temp. After washing with 5 ml PBS and centrifugation, the cell bound activity was measured. Mean binding of antibody to fixed and live cells was comparable with anti-p97 Mab (77%) and Fab (70%) and anti-proteoglycan Mab (51%) and FAB (20%) while binding to a non specific Mab was low (6%) and Fab (2%). Binding of anti-GD3 Mab was exceptional since fixed cell binding (69%) was much higher than live cell binding (28%), suggesting that fixation exposed additional antigenic determinants. Fixed cells can be stored for at least 6 months without loss of antigenic binding capacity. We conclude that cloned, fixed cells offer a stable, convenient reagent for testing the immunoreactivity of chemically modified anti-melanoma antibodies or fragments prepared for research or clinical applications.

(Supported by CA-29639-USPHS).

**Evaluation of Brain Tumor Immunolocalization in Relation to Resected Sample Radioactive Tracer Analysis.** R.B. Richardson, A.G. Davies, S. Bourne, J.T. Kemshead, and H.B. Coakham. *Frenchay Hospital, Bristol and Imperial Cancer Research Fund, London, UK*

We have investigated the ability of radiolabeled monoclonal antibodies specific for neuroectodermal tissue (UJ13A) and a nonspecific monoclonal antibody (HMFG2) to cross the blood-brain barrier and specifically localize in primary cerebral tumor. After a simultaneous i.v. injection of iodine-131 ($^{131}$I) UJ13A and iodine-125 ($^{125}$I) HMFG2, scintigraphy was then carried out at fixed time intervals up to 10 days. The maximum scintigraphic activity in the tumor occurred between 4–48 hr, with optimal visualisation from 1–5 days. There was increased uptake of monoclonal antibody in resected tumor compared with normal brain. However, the tumor uptake for specific and nonspecific antibody was approximately equal. In vivo antibody kinetics have been studied and we have also demonstrated the formation of immune complexes in certain cases, due to the presence of spontaneously occurring anti-mouse immunoglobulin.

We also report the successful localization in disseminated pineal tumor of $^{131}$I labeled monoclonal UJ181.4 directed against oncofetal neuroblastic antigen. The antibody was injected together with a $^{125}$I-labeled control antibody into the cerebro-spinal fluid (CSF) space. The results of immunoscintigraphy and radiolabeled antibody kinetics in the CSF, blood and urine confirmed specific localization of the anti-tumor agent. On the basis of this data, a therapy dose of 870 MBq of $^{131}$I-labeled UJ181.4 was given.

**Design for a Large Area Time-of-Flight Positron Detector.** M. Lichtenstein, G. Mack Jost, and T. Boal. *Royal Melbourne Hospital, Australia.*

An annihilation photon detector utilizing crossed arrays of liquid scintillator in glass light pipes or plastic scintillator light pipes is described.

The novel principle of this design is that Compton interactions in the primary light pipes produce light photons, 70% of which is absorbed by the adjacent secondary light pipes and then re-emitted at a higher wavelength (using a suitable secondary scintillator) with high (90%) efficiency.

Consequently, 15% of the primary light is delivered by total internal reflection to each end of the primary light pipe and the equivalent of 10% of the light output delivered to each end of the secondary light pipe. Geometric resolution is determined by primary light pipe diameter, hence resolutions of 3 mm are possible.

Because of the light piping and complexing of the ends of the light pipes, a detector area of 0.5 square meters can be imaged using 50 fast (time of flight) photo multiplier (PM) tubes for the primary light pipes, and 160 slow PM tubes for the secondary light pipes. This number allows reprocessing of up to four Compton interactions >50 keV per annhiliation photon. Total energy collection and Compton scatter analysis allows elimination of photons scattered in the patient.

Preliminary work has demonstrated that using 662 keV (Cesium-137) photons, 80% of photons reacting in the primary scintillator 2.5,diphenyl oxazole (PPO) light pipes are detected in the secondary scintillator 1:4 bis 2(5 phenyl oxazole) benzene (POPOP) light pipes.

Timing resolution of 700 psec was obtained using the above photons and a 20 cm long light pipe.

**Tomographic Brain Images Using a New Technetium-99m Labeled Oxime Pn-26 with Excellent Brain Retention.** A. Andersen, S. Holm, S. Vorstrup, O.B. Paulson, K. Kristensen, and N.A. Lassen. *Rigshospitalet, Copenhagen, Denmark.*

The technetium-99m-labeled propylene amine oxime PnAO freely crosses the blood-brain barrier. Its initial distribution in the brain as recorded over 10 to 20 sec by a rapidly rotating 4-camera SPECT (Tomomatic-64) is proportional to regional cerebral blood flow (CBF) measured by xenon-133 ($^{133}$Xe) tomography using the same instrument. As PnAO is not retained in the brain it is unsuited for conventional gamma camera. This paper concerns a new derivative $^{26}$Pn which is retained in the brain.

Six patients were injected i.v. by 17 to 40-mCi $^{99m}$Tc-labeled Pn-26. The early $^{26}$Pn images taken 15 to 26 sec after the injection showed $^{99m}$Tc in the tissue being proportional to CBF. Maximal count rate was recorded after 30–40 sec followed by a decrease in brain radioactivity to about half maximum over the following 10–15 min. From this time on and for at least 24 hr a state of permanent brain retention is evidenced by a constant image with a decay in count rate of 6 hr (the half-life of $^{99m}$Tc). This retention allows excellent tomographic imaging with much higher uptake in gray than in white matter, and with a spatial resolution of 12 mm. In particular the subcortical nuclei are much better seen than with $^{133}$Xe or iodine-123 IMP.

In normal man the images closely resembled the CBF distribution, but in patients with subacute stroke $^{26}$Pn shows a much higher uptake in peri-infarct areas than the low CBF would predict. This reveals enhanced regional extraction in these areas. Thus, despite the excellent retention $^{26}$Pn is not the perfect "chemical microsphere" for imaging CBF in cerebrovascular disease.

**Kinetic Analysis of IQNB and the Muscarinic ACh-Receptor System in Brain.** R. Blasberg, C. Patlak, S. Hiraga, K. Pettigrew, B. Francis, R. Gibson, R. Reba, S. Larson, and W. Eckelman. *George Washington University and NIH, Bethesda, MD.*

The distribution of the R- and S-quinuclidinyl derivatives of (RS)-1-azabicyclo[2.2.2]oct-3-yl (RS)-$\alpha$-hydroxy-$\alpha$-4-iodophenylacetate (IQNB) labeled with $^{125}$I was studied in 114 conscious rats after i.v. injection over experimental times ranging from 1 min to 26 hr. R-IQNB has been shown to have high affinity to cerebral muscarinic acetylcholine receptors, whereas the affinity of S-IQNB to these receptors is at least 100-fold less. Plasma and various tissues were sampled and the results analyzed by compartment (A) and graphical (B) methods. Preliminary estimates are:

| | A. $K_1\ k_2/(1 + K_{eq})$ | | B. $k_3/(1 + K_{eq})\ k_b$ | |
|---|---|---|---|---|
| | $\mu$l/gmin | l/min | l/min | l/min |
| Cortex | 0.25* | 0.14* | 0.040 | 0.0016 |
| Cerebellum | 0.26 | 0.059 | — | — |
| Cerebellum | 0.31* | 0.17* | — | — |

where the rate constants have the standard meanings ($k_b$ is the "loss" constant from the tissue) $K_{eq}$ is a reversible binding equilibrium constant, and the (*) indicates S-IQNB experiments. The log octanol/saline partition coefficient for IQNB was 1.6 and the single-pass capillary extraction fraction of IQNB in saline (Crone method) was 0.25. These preliminary results indicate that R-IQNB has selective binding characteristics in different brain structures, a slow but measureable "off-rate", and blood flow is *not* a determinant of the later images.

**Acetazolamide Enhancement of Regional Cerebral Blood Flow and HIPDm Flow Distribution Studies.** R. Burt, R. Reddy, H.N. Wellman, B. Mock, D. Schauwecker, and R. L. Roudebush. *Indiana University and VA Medical Center, Indianapolis, IN.*

We studied a series of patients with symptoms of cerebral vascular disease (CVD or TIA) with inhalation Xenon-133 regional cerebral blood flow measurements (rCBF) before and after i.v. administration of acetazolamide (Diamox) and SPECT imaging with HIPDm. Diamox is known to elevate rCBF in man and some animal species but the mode of action is unclear. It has been used with rCBF measurements to evaluate vascular reactivity; however, it apparently has not been used with HIPDm imaging. As expected, resting rCBF studies in asymptomatic TIA were usually normal, but most patients responded to Diamox with increases in rCBF of from 30 to 50%. An abnormal response was considered as little global response or focal areas of low response. HIPDm was given immediately after the second rCBF measurement and

within 20 to 25 minutes of Diamox. Areas of decreased uptake corresponding to the focal abnormalities of rCBF were easily seen and apparently discriminated differences of rCBF of about 10 ml/100 g/min for gray matter flow. Images after about 6 and 18 hr tended to normalize; however, these images were not optimal probably from low count statistics.

This preliminary data suggests that Diamox coupled with rCBF and HIPDm imaging may be a potent tool for detection of focal cerebral vascular disease. Delayed studies similar to cardiac thallium-201 ($^{201}$Tl) imaging may be feasible but it is likely a second HIPDm dose will be needed.

**A New Lipophilic Brain Scanning Agent: Preliminary Experience with Technetium-99m-Hexamethyl-PAO.** P.J. Ell, P.H. Jarritt, J.M.L. Hocknell, I. Cullum, and D.C. Costa. *The Middlesex Hospital Medical School, London, UK, and* D.P. Nowotnik, R.D. Pickett, R.D. Neirinckx, *Amersham International, UK.* W.A. Volkert, and R.A. Holmes.

Propyleneamineoxime can traverse the intact blood-brain barrier when chelated with technetium-99m ($^{99m}$Tc), but requires fast SPECT instrumentation for tomographic studies of the human brain due to its rapid cerebral clearance. A derivative of this compound, $^{99m}$Tc-hexamethyl-propyleneamineoxime ($^{99m}$TcHM-PAO) exhibits favorable properties for regional cerebral tomograms in man (rCBF) utilizing conventional instrumentation. The following data is available at present.

No toxic effects shown in rats at dose equivalent to 7,000 times the human dosage (0.125 mg); 20 mrad/mCi whole-body dose in man (base on rat biodistribution data); rapid blood clearance in humans (at 15 min p.i., less than 10% of injected activity present).

In man, at 20′, 45′, 60′, and 4.5 hr p.i., percent organ uptake in the brain is 3.9, 3.7, 3.7, and 3.5, respectively; in the liver, 25.3, 23.5, 22.4, and 21.8; and in the urinary bladder 2.4, 3.9, 5.1, and 8.3%. At 24 hr, whole-body retention is ~70% of total activity.

Conventional studies were undertaken with an IGE400A rotating gamma camera and a multidetector tomographic brain scanner (Cleon 710). So far, a total of 22 human studies have been performed. In ten, x-ray CT and $^{123}$I-isopropyl-amphetamine (IMP) comparative data are available. Established stroke is clearly seen, with similar or superior detail, when compared with IMP.

**Thallium-201 DDC, an Alternative to Iodine-123 IMP.** E.A.V. Royen, J.F. de Bruïne, A. Vyth, Th.C. Hill, J.M.B.V. de Jong, J.B. van der Schoot. *Academic Medical Center, Amsterdam, and the Deaconess Hospital, Boston, MA.*

The high cost and limited availability of iodine-123 ($^{123}$I) iodoamphetamine ([$^{123}$I] IMP) led us to search for alternative lipophilic radiopharmaceuticals in the study of brain perfusion.

Thallium-201 [$^{201}$Tl] diethyldithiocarbamate ([$^{201}$Tl] DDC) is an easy to prepare highly lipophilic complex with considerable brain uptake in the rat (Vyth et al: *Pharmacol Week Sci Ed* 5: 213, 1983). In rabbit 1.46% ± 0.28 s.e.m. of [$^{201}$Tl] DDC was taken up by the brain compared with 1.14% ± 0.28 s.e.m. of [$^{123}$I] IMP. The ratios of gray and white matter distribution were equal. No lungretention was found for [$^{201}$Tl]DDC. The kinetics of brain uptake of [$^{201}$Tl]DDC demonstrated a faster uptake and a more instantaneous equilibrium, 1.5 min. after injection, than [$^{123}$I] IMP. Macroautoradiography of the brain showed a clear demarcation of gray and white matter, stable for at least 1 hr.

The favorable properties of [$^{201}$Tl]DDC prompted us to investigate its use in human volunteers as a new radiopharmaceutical for single photon emission computed tomography (SPECT) imaging of brain perfusion. After the injection of 3 mCi $^{201}$Tl DDC whole-body images, plain gamma camera images as well as rotating gamma camera were acquired. Tomographic images representing brain perfusion, proved to be satisfactory. Employing the Harvard Multidetector brain system, high quality images similar to [$^{131}$I] IMP cerebral blood flow images were obtained up to 3 hr after injection.

Thallium-201 DDC SPECT may find widespread clinical application in acute cerebral ischemia due to its general availability.

**The Role of Scintigraphy in Chemotherapy of Brain Tumors Using Induced Blood-Brain Barrier Disruption.** G.J. Wang, R.A. Holmes. *Nuclear Medicine Section, University of Missouri, Columbia, MO.*

Increasing longevity of patients with malignant brain tumors is the objective of mannitol induced regional blood-brain barrier disruption (BBBD). The procedure enhances the delivery and tumor concentration of chemotherapeutic drugs practially eliminating the failure of systemic chemotherapy that does not avidly localize in the tumor. To clearly define the regional distribution of the BBBD planar radionuclide brain imaging has been shown to be effective without the adverse side effects of angiography. With our neurosurgeons, neurologists and neuroradiologist we have initiated an ongoing protocol of serial BBBD chemotherapy in patients with progressive malignant brain tumors. Following surgery and irradiation patients showing tumor progression clinically and documented with x-ray computed tomography (XCT) are placed on the protocol consisting of intravenous cytoxan (20–30 mg/kg) followed by selected internal carotid or vertebral artery infusion of hypertonic mannitol and the administration of methotrexate (1–3 gm) and 20 mCi technetium-99m diethylenetriaminepentaacetic acid intravenously. Multiview brain images are taken 3 hr later. In the first 11 patients 45 BBBD have been performed. Three failed for various reasons while 42 demonstrated excellent disruption scintigraphically. Tumor response and the need to repeat the BBBD are evaluated monthly by XCT. Patients have averaged nearly four BBBD's (range 2–7). To date two patients have expired and the mean survival in this group has been 167 days. Few complications have been observed and these initial results appear very promising.

**Phosphorus-31 Nuclear Magnetic Resonance Spectroscopy of Human Prostate Tumors In Vivo.** G.D. Clarke, P.P. Fatouros, R. Raynor, J. Montour, and P.R.S. Kishore. *Medical College of Virginia, Richmond, VA.*

The phosphorus-31 ($^{31}$P) nuclear magnetic resonance (NMR) surface coil spectroscopy technique has been widely applied to the noninvasive monitoring of the concentrations of

high-energy phosphate metabolites in various tissues. This technique has great potential in the study of biochemical changes in malignant tissue within the context of the host environment. Phosphorus-31 NMR spectra were obtained from prostate tumors induced in Balb/c immunodeficient mice. $10^7$ cells of the human prostate line, PC3, were injected subcutaneously into the right flanks of these animals, and palpable tumors were evident within 7–10 days at the injection site. The spectra were obtained at 1.89T using a three-turn conical spiral surface coil (0.8 cm outer diam) which was coated with Teflon to insulate the conductor from the tissue. Spectra were also obtained from the left flanks of the animals which served as controls.

The relative concentration of phosphocreatine was found to decrease with time as the tumor grew while the relative concentrations of inorganic orthophosphate and the sugar phosphates increased. Relatively rapid changes in the metabolite concentrations and intracellular pH (as measured from the chemical shift between phosphocreatine and inorganic orthophosphate) occurred as a result of exposure to x-irradiation (14 Gy, 250 keV, single dose). These results show that $^{31}P$ NMR spectroscopy can be useful for studying the metabolic properties of malignant tissues in vivo.

**Indication of Doxorubicin Induced Impairment in Fatty Acid Utilization.** R. Dudczak, R. Lenzhofer, and K. Kletter. *1st Medical Clinic, University of Vienna, Austria.*

The aim of the present study was to evaluate in rat experiments if doxorubicin (D) may impair fatty acid utilization. We studied the utilization of 15-*p*-$^{131}$I-iodophenylpentadecanoic acid (PPA) in rat hearts using TLC of homogenized heart extracts. About 50 $\mu$Ci [$^{131}$I]PPA was given i.v. in either untreated rats (Co) or those having received 20 mg/kg D intraperitoneally 24 hr (24D) or 48 hr (48D) previously. Each group consisted of six Sprague Dawley rats. The hearts were rapidly removed 1 min after i.v. [$^{131}$I]PPA, frozen in liquid nitrogen, weighed and counted. Iodine-131 radioactivity distribution in hearts was determined after lipid extraction and thin layer chromatography (TLC). In additional rat experiments (12 rats/group), high energy phosphates and carnitine were determined enzymatically in heart extracts.

The mean PPA uptake (% dose/g) was 2.49 in Co, 1.74 in 24D, and 2.36 in 48D rats. Usually five peaks were separated by TLC, one with an Rf value of 0.29 ± 0.03 corresponding to PPA and the remaining four to catabolites of PPA metabolic breakdown. The mean relative amount of unmetabolized PPA as compared to the fractions of PPA catabolites was less in Co than in 24D or 48D rats ($\bar{x}$: 46.5% compared with 72.4% compared with 59.4% resp.; $p < 0.05$). The mean carnitine content of heart extracts was higher in Co (0.69 $\mu M/g$) than in D treated rats (24D: 0.51 $\mu M/g$; 48D: 0.54 $\mu M/g$) ($p < 0.05$). The total amount of high energy phosphates was not different between the groups. However, the mean ATP/AMP ratio was higher in Co (35.9) than in 24D (22.3) or 48D (27.1) rats.

Our findings show for the first time, that D causes a reversible impairment in PPA utilization, possibly mediated by carnitine deficiency. Thus, PPA might be useful in patients on D therapy to evaluate eventual D induced effects on myocardial fatty acid metabolism.

**Evaluation of Cobalt-57 Tipped Biopsy Needle for Fine Needle Biopsy Under Scintigraphic Control.** K.S. Subramanian, D.L. Bushnell, E.L. Kanabrocki, M.L. Freeman, and E. Kaplan. *Veterans Hospital, Hines, IL.*

Scintigraphic guidance of tissue needle biopsy (TNP) has many potential clinical applications. The study was undertaken to evaluate the usefulness of cobalt-57 ($^{57}$Co) tipped biopsy needle in TNP of lesions which are either hot or cold when imaged with technetium- ($^{99m}$Tc) labeled radionuclides. Cobalt-57 decays by electron capture with a physical half-life of 270.9 days, mean energy of the abundant gamma radiation being 122.1 keV (85.5%). The first 5 mm of the tip of ten spinal needles were coated with $^{57}$Co and overlayed with a stable cobalt isotope. The activity at the tip ranged from 3.3 to 17.1 $\mu$Ci. The needles were tested for firmness of adhesion by a simple wipe test and multiple sequential perforations of store purchased meat. The needles were imaged in both cold and hot nodules of a thyroid phantom filled with about 500 $\mu$Ci of [$^{99m}$Tc]pertechnetate using a high resolution pinhole collimator. All needles were well visualized in the cold nodules at energy peaks of 122, 130, and 140 keV, with a window setting of 10%. The needle with 17.7 $\mu$Ci of $^{57}$Co activity at the tip could be detected in the hot nodule at energy peaks of 133 and 120 keV, with a window setting of 10%. An anesthetized dog was injected with 2 mCi [$^{99m}$Tc] sulfur colloid and placed under a gamma camera with a low-energy, all-purpose, collimator. By scintigraphically visualizing the liver in two projections (anterior and right lateral) using a persistance scope, the needle with 17.7 $\mu$Ci of $^{57}$Co activity at the tip was easily maneuvered into various anatomic locations of the liver at an energy peak of 130 keV and a window setting of 10%. Cobalt-57 tipped needles can be especially useful in TNP of bone and deep brain lesions where ultrasound guidance is not applicable.

**Synthesis of Indium-111 Porphyrins and Their Biodistribution in Hamsters Bearing Transplanted Malignant Melanomas.** N. Foster, D.V. Woo, F. Kaltovich, J. Emrich, C. Ljungquist, S. Hemperly. *Lehigh University, Bethlehem, PA, and Hahnemann University, Philadelphia, PA.*

Cationic, water-soluble complexes of indium-111 ($^{111}$In) and three synthetic porphyrins (tetra 4-*N*-methylpyridyl porphyrin [T4NMPyP], tetra 3-*N*-methylpyridyl porphyrin [T3NMPyP], and tetra *N,N,N*-trimethylanilinium porphyrin [TMAnP]) have been prepared, purified and evaluated at 6, 24 and 48 hr postinjection for tumor uptake in Syrian Golden hamsters bearing flank-transplanted malignant melanomas (Fortner MMI). Statistical treatment of the biodistribution data shows that the two isomeric pyridyl porphyrins experience the same biodistribution in tissues and selective concentration in the melanoma; at 6 hr postinjection of [$^{111}$In] T4NMPyP the amount of activity in the tumor exceeds that in all other organs (tumor-to-blood = 43:1). Liver, spleen, and lung show lower organ-to-blood ratios at all time points compared to tumor. The distribution of the anilinium porphyrin is statistically different, showing higher organ-to-blood ratios for kidney, liver, and spleen than for tumor at all time points and higher activity levels in all tissues compared to the pyridyl porphyrins. Gamma camera images of hamsters injected with $^{111}$In T4NMPyP and TMAnP illus-

trate these differences as well as another phenomenon of selective uptake of $^{111}$In T4NMPyP also verified in biodistribution data: 20 times as much activity concentrates in the viable periphery of the tumor compared to the amount in the necrotic core. Indium pyridyl porphyrins demonstrate considerable promise as agents to aid in the diagnosis and evaluation of malignant melanotic disease.

**Brain Protein Synthesis Rates Measured In Vivo Using Methionine and Leucine.** R.M. Jones, S. Cramer, T. Sargent, T.F. Budinger, *Donner Laboratory, Lawrence Berkeley Lab, and University of California, Berkeley, CA.*

Interpretation of positron emission tomography (PET) accumulation data from carbon-11- ($^{11}$C) labeled amino acids depends on knowledge of the metabolic fate of the label. These experiments measure the relative amount of label in different metabolic products as a function of time after injection of carboxy-labeled leucine or methyl-labeled methionine.

Rats were injected i.v. with carboxy-[$^{14}$C]-labeled leucine or methyl-[$^{14}$C]-labeled methionine. Labeled metabolites were separated and measured in blood and in brain extracts with high performance liquid chromatography, thin layer chromatography, and by specific biochemical assays. Protein in blood and brain was separated by acetonitrile precipitation and basic hydrolysis before counting the amount of label incorporated.

The methyl-label of methionine went to a number of non-protein metabolites, including: S-adenosylmethionine (18%), sarcosine (7%), serine (3%), glycine (1%), phospholipids (5%), and bicarbonate (2%), these comprising up to 36% of total activity in brain at 45 min after injection. The minor metabolites of leucine (alpha-keto-isocaproic acid and bicarbonate) constituted less than 3% of the activity in the rat brain at the same time.

Leucine provides a better measure of brain protein synthesis rates measured with PET or autoradiography, primarily because leucine was found to have fewer side reaction products than methionine. For leucine, the blood input and brain uptake data can be fit to a simple three compartment kinetic model to estimate the local rate of brain protein synthesis.

**Fluordecarboxylation with Fluorine-18 Fluoride Ion/Xenon Difluroide: A New Route to Fluorine-18 Radiopharmaceuticals.** T.B. Patrick, M.R. Kilbourn, and M.J. Welch. *Mallinckrodt Institute of Radiology, Washington University School of Medicine, St. Louis, MO.*

Xenon difluoride reacts with aliphatic carboxylic acids to effect replacement of the carboxyl group by fluorine (Patrick et al: *J Org Chem* 48, 4158, 1983). This process, termed fluorodecarboxylation, provides alkyl fluorides in high chemical yields. We have found that the inclusion of fluorine-18 ($^{18}$F), in the form of tetrabutylammonium [($^{18}$F)] fluoride, in a normal fluorodecarboxylation reaction results in formation of $^{18}$F-labeled alkyl fluorides in high radiochemical yields. Two examples are shown below. The proposed reaction mechanism involves reaction of the acid with the xenon difluoride to form a xenon fluoride ester, RCOOXeF, which undergoes nucleophilic attack by fluoride ion. In situ formation of $^{18}$F-labeled xenon difluoride does not occur. This represents a new and simple method for carrier-added synthesis of $^{18}$F-labeled alkyl fluorides, and its use in the preparation of $^{18}$F radiopharmaceuticals is under study. The use of the [$^{18}$F]-fluoride ion/xenon difluroide reagent for aromatic fluorinations appears similarly promising, and examples will be presented.

$$BrCH_2CH_2CH_2COOH + XeF_2 + {}^{18}F^- \rightarrow BrCH_2CH_2CH_2{}^{18}F \quad (78\%)$$

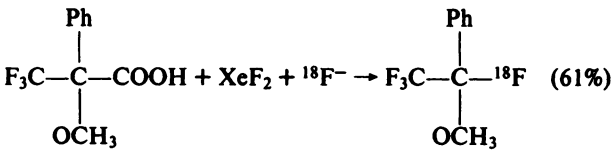


**The Labeling of Bovine Endothelial Cells in Monolayer with Indium-111.** K. Ramberg, R. Hanson, R. Connolly, W. Baur, A. Callow, and P. Kahn. *Tufts-New England Medical Center and Northeastern University, Boston, MA.*

This study compared uptake kinetics and labeling efficiencies of two preparations of indium-111 ($^{111}$In) oxine and [$^{111}$In]tropolone for bovine endothelial cells in monolayer.

The cells were seeded onto six-well plates and grown to confluence (2-3 days). The media with serum was removed, the cells washed once with serum-free media, and serum-free media added as the labeling solution. The cells were incubated with [$^{111}$In] oxine in ethanol (IOE), [$^{111}$In] oxine in saline (IOS), or [$^{111}$In]tropolone (IT) for 5, 15, 30, or 60 min. After incubation the cells were enzymatically harvested, assayed for radioactivity, and tested for viability by vital dye exclusion. Results are shown below.

Labeling efficiencies (% ± s.e.m.)

| min | IOE | IOS | IT |
|---|---|---|---|
| 5 | 28.9 ± 3.1 | 31.8 ± 2.2 | 10.7 ± 1.1 |
| 15 | 49.3 ± 2.4 | 54.8 ± 5.7 | 20.7 ± 1.9 |
| 30 | 64.0 ± 5.0 | 65.4 ± 4.1 | 24.8 ± 3.3 |
| 60 | 67.3 ± 5.6 | 71.4 ± 10.4 | 36.4 ± 3.2 |

Although the IOS produced consistently higher labeling efficiencies than IOE the difference was not significant. Indium-111 tropolone had significantly decreased labeling efficiencies when compared to [$^{111}$In] oxine. Viability was not affected by the labeling.

Preliminary data suggests that labeling efficiencies with [$^{111}$In]tropolone are comparable to those of [$^{111}$In]oxine when saline is used as the labeling solution.

(Supported by NIH Grant HL28855.)

**Animal Studies Using $^{67}$Cu-Labeled Meso Tetra(4-Carboxyphenyl) Porphine.** Z.V. Svitra, P.M. Wanek, J.A. Mercer-Smith, W.A. Taylor, and F.J. Steinkruger. *Los Alamos Medical Radioisotope Research Group, Los Alamos National Laboratory, Los Alamos, NM.*

Conjugation of chelating agents with appropriate proteins is an important method of labeling monoclonal antibodies.

Radioactive emissions of copper-67 ($^{67}$Cu) have a potential for being useful in delivering lethal radiation to cancer cells as well as for imaging purposes. For this method, a porphyrin ligand was metalated which has a high binding affinity for $^{67}$Cu and thus should survive in vivo. The porphyrin also has carboxylate groups for conjugation to proteins.

In this preliminary study, we examined the biodistribution, imaging, and biological half-life of $^{67}$Cu labeled meso-tetra(4-carboxyphenyl) porphine ([$^{67}$Cu]TCPP). Biodistribution studies were performed using normal male Fisher 344 rats 1 hr, and 1, 2, 3, 4, and 5 days after tail vein injections. Tissue samples, carcass, and waste were counted for activity using either a NaI well counter or the Packard Auto-Gamma Scintillation Spectrometer. Activity balances averaged 97%. Images of three animals were obtained showing substantial $^{67}$Cu activity in the liver, kidneys, and gut. This was corroborated in the biodistribution work. In animals with known infections, substantial uptake in lymph nodes was noticed. A model study of this phenomenon is in progress. The biological half life appears to be a biphasic elimination.

(Research supported by U.S. Department of Energy and Office of Health and Environmental Research.)